Analysis and control of a vehicle with variable torque distribution

Analysis and Control of a Vehicle with Variable Torque Distribution

S.T.M. Bus

DC 2014.054

Traineeship report

Coach(es): Josef Duernberger (Daimler AG)

Supervisor: prof.dr. H. Nijmeijer

Technische Universiteit Eindhoven
Department Mechanical Engineering
Dynamics and Control Group

Eindhoven, November, 2014

Abstract

Consider a vehicle where one can distribute the drive or brake torque with every desired percentage between its front and rear axles. What is the potential of such a system with regards to the cornering performance? In this document this is investigated with simulations from a full vehicle model. The combined behavior on the limit (right before the vehicle becomes unstable) and at lower lateral acceleration under certain longitudinal acceleration/deceleration is of special interest. This is investigated at certain road friction levels, in order to get the influence of the road/tire contact. Ultimately, it appears that on the limit of friction a vehicle that has such a system can perform better in a corner than one without. However, in some situations the vehicle can become unstable in an undesired way (i.e. oversteering). When that happens, it is better to choose a distribution that reaches a slightly lower lateral acceleration. For the lower longitudinal acceleration it does not appear to differ much. Finally, a controller is developed that influences the steering behavior of a vehicle using the distribution. This controller was tested by several test drivers on the driving simulator and could improve the stability and driveability of the vehicle especially under bad road conditions. This was proven by simulations on the vehicle model as well.

Nomenclature

List of symbols

α	Sideslip angle	$[^\circ]$
a	Acceleration	$[\mathrm{m/s^2}]$
β	Vehicle sideslip angle	$[^\circ]$
c	Stiffness (gradient)	
δ_{LRW}	Steering wheel angle (angle of the steering wheel)	$[^\circ]$
δ_s	Wheel steering angle (total angle of the front wheel)	$[^\circ]$
e	Error	$[-]$
EG	Understeer gradient	$[^\circ/(\mathrm{m} \cdot \mathrm{s}^2)]$
F	Force	$[\mathrm{N}]$
i_L	Reduction factor between steering wheel angle and wheel steering angle	$[-]$
κ	Longitidunal slip	$[-]$
L	Length	$[\mathrm{m}]$
μ	Friction level	$[-]$
ψ	Yaw angle	$[^\circ]$
R	Radius	$[\mathrm{m}]$
SG	Vehicle sideslip gradient	$[^\circ/(\mathrm{m} \cdot \mathrm{s}^2)]$
T	Torque	$[\mathrm{N} \cdot \mathrm{m}]$
t	Time	$[\mathrm{s}]$
V	Speed vector	$[\mathrm{m/s}]$
v	Speed	$[\mathrm{m/s}]$
ξ	Distribution	$[-]$

List of indices

CoG	Center of gravity
c	Constant
HA	Defined from rear axle
hor	Vectorial absolute
hl	Rear left
hr	Rear right
max	Maximum
PI	Signal coming from PI controller
RA	Rear axle
ref	Reference
t	Current time
vl	Front left
vr	Front right
x	Longitudinal axis
y	Lateral axis
z	Vertical axis

Contents

Chapter 1

Introduction

In this chapter, first the project description is stated. After that, the vehicle model that is used is explained. Then the goal, scope and used method of this research are stated. Finally, the structure of this document is made clear.

1.1 Project description

In this project a vehicle with the ability to freely distribute the driving or braking torque between the front and rear axle is considered. The division between the axles is called ξ_{HA}.

The goal here is to investigate first the effect of being able to control, real-time, the distribution of torque. Therefore, two driving regions are of main interest:

- The linear region of the tyre to investigate the under- and oversteering characteristics of the vehicle.
- The limit (non-linear) region where the stability and maximum cornering performance are analysed (friction circle).

To investigate this, manoeuvres with combined longitudinal and lateral accelerations are used.

Furthermore, it should be investigated how a ξ_{HA} controller can influence the friction circle and make optimal use of it. Based on the results of the constant distribution a controller should be developed, which should use the potential of such a vehicle with variable drive force distribution. This controller will be tested in a driving simulator and, if necessary, adjusted according to the results.

1.2 Description of the system

We consider a vehicle that is able to freely change its distribution of drive or brake torque between its front and rear axles. So, for a given drive torque T_{drive}, one can choose to apply a certain percentage of that torque on the front axle and the rear axle. ξ_{HA} is defined as:

$$\xi_{HA} = \frac{T_{rear}}{T_{front} + T_{rear}} \tag{1.1}$$

Here, T denotes the driving torque on either the front or rear axle.

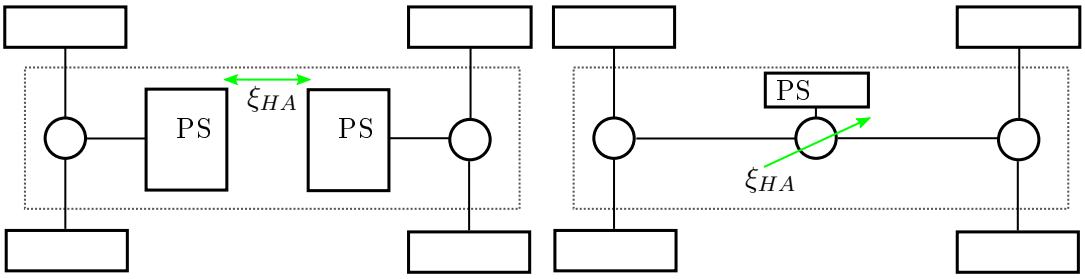

(a) Two independent power sources (b) Variable central clutch

Figure 1.1: Two possible forms of a vehicle with variable torque distribution
PS = Power Source

Thus, if ξ_{HA} equals 1 the vehicle is rear wheel driven, whilst for $\xi_{HA} = 0$ the vehicle is fully front wheel drive. This is the same for both driving and braking. For example, a distribution of 20% means that braking will also happen with 20% on the rear axle.

In conventional vehicles the brake torque distribution is fixed by the hydraulic braking system. For hybrid or electric vehicles this is usually changed within limits. The axles for mechanical all-wheel drives are coupled by a differential with a fixed ratio (without limited slip) or by a clutch. Thus their torque distribution can not be changed independently from each other. In the case that is considered here there are two independent power sources that can apply braking and driving torques and thus give the maximum freedom of distribution.

To distinguish this project from torque vectoring investigations, it has to be mentioned that torque vectoring usually focuses on the left to right torque distribution, whilst here the distribution between two axles is the only degree of freedom. Hence, since no limited slip differentials on the axles are considered the following is valid:

$$\begin{aligned} T_{front} &= \frac{1}{2}T_{front,left} + \frac{1}{2}T_{front,right} \\ T_{rear} &= \frac{1}{2}T_{rear,left} + \frac{1}{2}T_{rear,right} \end{aligned} \tag{1.2}$$

The vehicle with a variable torque distribution can be a hybrid vehicle, but does not necessarily need to be. In Figure 1.1 two different forms of such a vehicle are shown.

Figure 1.1a shows a vehicle which has two power sources. This can of course be any combination of either electric or conventional power sources. Here, the desired torque is divided between the two sources according to the set distribution. What distribution ξ_{HA} to apply and when is discussed later in this report. Secondly, there is the type of set-up as shown in Figure 1.1b. This vehicle has one power source, which is connected via one clutch, multiple clutches or a limited slip differential to the driveline. A vehicle with one clutch has one axle permanently connected, and, using the clutch, can connect the other axle. With this system, there is a limitation since the first axle cannot be decoupled. When a limited slip differential is employed both axles are coupled permanently, and a distribution is possible according to the wheel speed differences. The limited slip differential balances the different speeds of the two output axles, and therefore a totally free distribution is not possible.

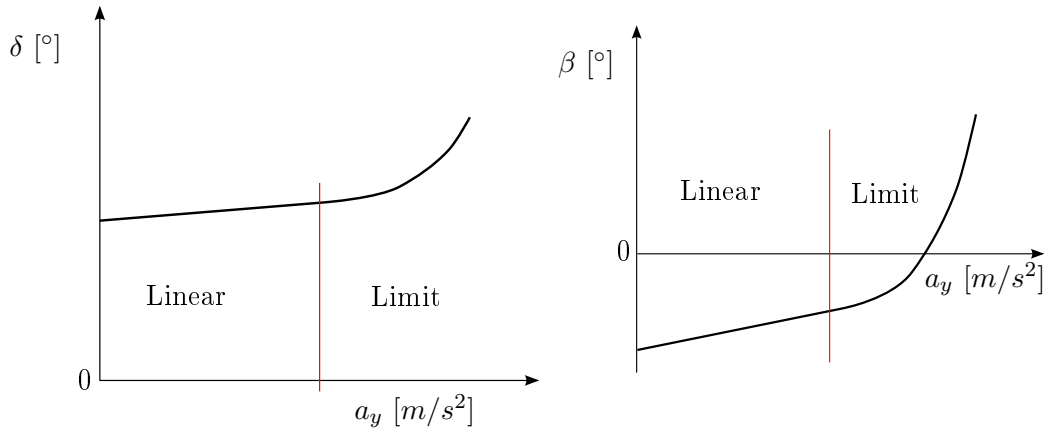

(a) Steering angle δ versus lateral acceleration a_y

(b) Vehicle side slip angle β versus a_y

Figure 1.2: Overview of the two regions of interest

1.3 Goal and scope of research

The goal of this research is to investigate the potential of such a system, where driving torques can be distributed freely. Of special interest is the self steering behavior of the car, and the behavior at the friction limits. The methodology is based on simulations done with an extensive full vehicle model. Furthermore, a controller is developed for ξ_{HA}. This controller is also tested in a driving simulator.

As stated above, for the simulations, two regions of operation are of interest. The first is the limit region, which gives the behavior of the vehicle at the friction limit. This means that the lateral and/or longitudinal accelerations are high and approaching the outer limit of the friction circle.

The second region is the linear region. Here, the lateral and longitudinal accelerations are both low, and care is taken that the limit is not approached. The name already implies that the linear behavior of the vehicle is of interest. This includes the understeer gradient and the vehicle sideslip angle gradient.

In Figure 1.2 a graphical overview of the two regions of interest is shown. From this figure, it can be seen that the linear region is where δ and β increase or decrease linearly with increasing lateral acceleration a_y. At a higher a_y, the linear behavior is changing from linear to a more and more non-linear behavior. If the lateral acceleration is even more increased, the vehicle becomes unstable. It is defined that the vehicle is unstable when the values of longitudinal slip κ on at least one wheel or the vehicle side slip angle β becomes too high. When κ is too high, the wheel is unstable and this can lead to complete instability of the vehicle.

At this limit the maximum a_y for a certain a_x and a certain ξ_{HA} is reached. This is then the limit for that particular vehicle with some distribution ξ_{HA}.

Since the vehicle behavior under combined longitudinal and lateral acceleration is of interest, there are certain longitudinal driving or braking forces F_x applied to the front and rear axle according to ξ_{HA}. For the front axle this force is denoted by $F_{x_{front}}$. Similarly, the force on the rear axle is denoted by $F_{x_{rear}}$. These two can be plotted against each other to show the relationship

between them. In Figure 1.3 such an F_x plot is shown. We can define four sections in this graph. When both front and rear are positive, the vehicle is driving. When both are negative, the vehicle is braking. If one is positive and the other is negative, this means that one axle is driving the vehicle and the other axle is counteracting this. For a vehicle with one power source per axle, this could mean that one axle is braking regeneratively. The vehicle is then charging its batteries via the street. For a vehicle with only one power source, it is not feasible to create different signs of F_x between the axles since there is only one power source. The red line shows a front wheel driven car, whereas the blue line depicts a rear wheel driven car. For a fully front wheel driven car, $F_{x_{rear}}$ is of course zero. Analogous to this, for a rear wheel driven car the longitudinal driving force on the front axle is zero. Furthermore, the black line shows $a_x = 0$. Since the longitudinal forces are then exactly opposite, the total force F_x is zero, and there is thus no acceleration in the longitudinal direction.

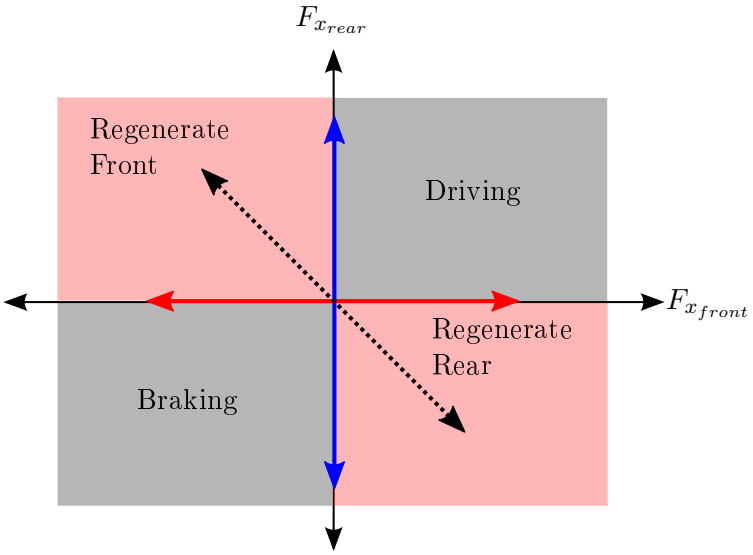

Figure 1.3: Four quadrants of operation with respect to longitudinal force F_x on the axles. The dotted line represents $\sum F_x = 0$

For a system that can vary the distribution between the two axles freely, the operating points can lie anywhere in this plane. Here, only the 'Driving' and 'Braking' quadrants are of interest. This means that the regenerative quadrants are outside the scope of this project.

1.4 Used method

This investigation is performed with simulations on a full vehicle model equipped with this system. This model includes (amongst others) weight transfer over both lateral and longitudinal axes, (elasto-)kinematics of the suspension and a Magic Formula tyre model. The simulations need to be performed with different longitudinal and lateral accelerations, a_x and a_y, respectively. This can be done by performing several simulations and varying the accelerations. For example, both a_x and a_y are varied between 1 and 3 $\mathrm{m/s^2}$ with steps of $1\,\mathrm{m/s^2}$. To investigate these situations, then $3 \times 3 = 9$ simulations are needed. When more maneuvers are investigated

the amount of simulations will become too high. Furthermore, it is then difficult to find the limit of friction, since each simulation is performed stationary.

Because of the aforementioned reasons, it is chosen to perform the maneuvers in a quasi-stationary manner. This means that a sweep with respect to a_y is performed by letting the vehicle accelerate in a corner. This is done with a fixed radius or with a linearly increasing steering wheel angle, both coupled with a fixed a_x. Which method (steering wheel angle or radius) is used is dependent on the situation and further on explained in other chapters. With this quasi-stationary method, in previously mentioned example only 3 simulations would be needed for the three different a_x.

The simulations with different longitudinal accelerations together with the different distributions form data as to how the vehicle behaves. The used representation of this data for the limit region is the friction circle. This graph shows the maximum reachable lateral acceleration for the different longitudinal accelerations. How the friction circle is obtained is explicated further on in Chapter 2. For the linear region the steering wheel angle and vehicle side slip angle versus lateral acceleration are of importance (both with different distributions). How these figures are obtained is explained in Chapter 3.

1.5 Outline of this document

This document is built up as follows. First, the investigation on the limit region is explained in Chapter 2. In this chapter, we explain the maneuver used to determine the friction circle for the vehicle. Then, the results of the investigation are shown and discussed. In Chapter 3 we first explain the maneuver used to investigate the linear region. The results are then discussed and explained. Finally, a conclusion with respect to the potential of a variable torque distributing system for the linear and limit region is drawn. Based on this, a controller to control the distribution of torque is designed in Chapter 4. The test results, for both testing on the vehicle model and in a driving simulator, are discussed and possible improvements are formulated. Finally, in Chapter 5 a summary is made of what is discussed in this document.

Chapter 2

Limit region

In this chapter, the goal of the limit region investigation is explained, as well as the maneuver that is used to generate the friction circle. Then the results of simulations are explained for different friction levels of the road. After that, conclusions are drawn.

2.1 Introduction

Here, the goal is to obtain an insight in how the vehicle will behave at the limits of friction under different distributions. The best way to visualize this behavior is to plot the limits in a friction circle. The friction circle shows the boundaries within which a vehicle remains stable.

For a given longitudinal acceleration a_x, specific for the maneuver performed, the lateral acceleration a_y is increased. This is done by applying a steering wheel ramp δ_{LRW}. This causes the vehicle to drive a certain radius R. Note that only the steering wheel input is controlled, so R is not constant nor does it change in a specific manner. With an acceleration in the longitudinal direction, an increasing acceleration in the lateral direction is achieved, even if the steering wheel angle is kept constant. The lateral acceleration is increased until the vehicle becomes unstable.

We define a combined acceleration, the absolute value of the lateral and longitudinal acceleration, a_{hor}:

$$a_{hor} \equiv \sqrt{a_x^2 + a_y^2} \ [\mathrm{m/s^2}] \tag{2.1}$$

The combined acceleration is needed to determine the outermost point on the friction circle. It can be seen from Figure 2.1 that the point where a_{hor} is the highest, that this is the point furthest away from the origin.

This procedure is done for several a_x, recording each a_y at the point where a_{hor} is the highest. In Figure 2.1 is a schematic overview shown of this. If this sweep over the longitudinal accelerations is repeated for several ξ_{HA} the different friction limits for the corresponding distributions can be created.

This is the theoretical basis to obtain the friction circle. Of interest is the behavior of the vehicle under low longitudinal accelerations and whether or not the distribution has any effect on the cornering performance and stability there. Furthermore, it is important to know how the vehicle will behave on the limit or close to it: will it understeer or oversteer? In the following the used maneuver is explained, as well as the results for the limit region.

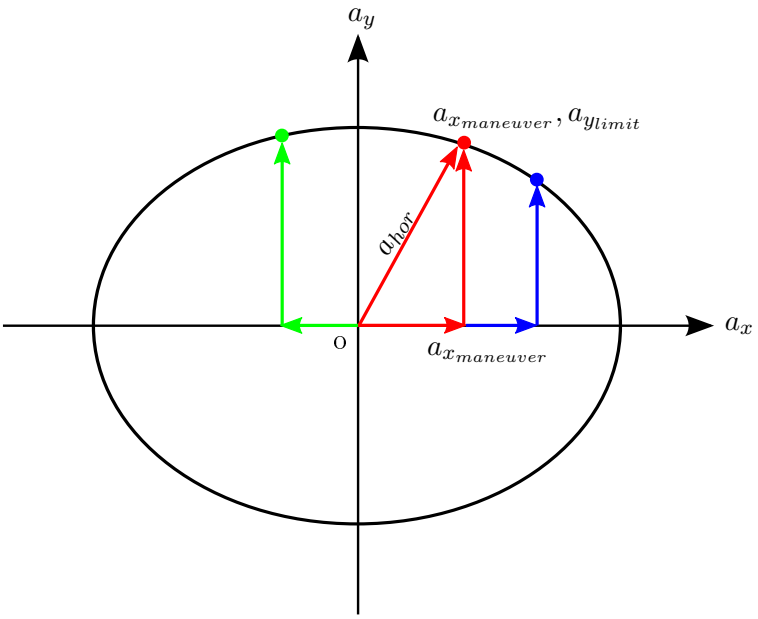

Figure 2.1: Schematic overview of the strategy to obtain the friction circle for one distribution

2.2 Used maneuver

The front steering angle, denoted by δ_s, is related to the steering wheel angle δ_{LRW} as follows:

$$\delta_s = \frac{1}{i_L}\delta_{LRW} \tag{2.2}$$

LRW stands for Lenkradwinkel, which is German for steering wheel angle. Here, i_L is assumed to be constantly 15.5. In reality, however, this factor is variable depending on several different factors.

In Figure 2.2 the steering wheel angle δ_{LRW}, longitudinal and lateral acceleration are displayed for this maneuver. This is an example for one of many performed maneuvers for one distribution. The full friction circle was obtained by performing several different longitudinal accelerations and using different distributions.

In chronological order, first a longitudinal acceleration is applied. To avoid instability, this is done gradually with a ramp. In this case, the jerk was about $4\,\mathrm{m/s^3}$. After 3 seconds the steering wheel angle δ_{LRW} is increased until the vehicle becomes unstable. In this case, this happens around $48°$ steering wheel input. In the end, the lateral acceleration reached is $5.1\,\mathrm{m/s^2}$ and the longitudinal acceleration is $4\,\mathrm{m/s^2}$. At that point the horizontal acceleration a_{hor} is the largest, so in this example this point would be saved for the friction circle.

What causes the instability of the vehicle is also of importance. The simulation is stopped when the vehicle side slip angle β becomes too large (more than $5°$), or when the longitudinal slip on one or more wheels becomes greater than 10%.

For both parameters it applies that above a certain value the linear region transfers into a non-

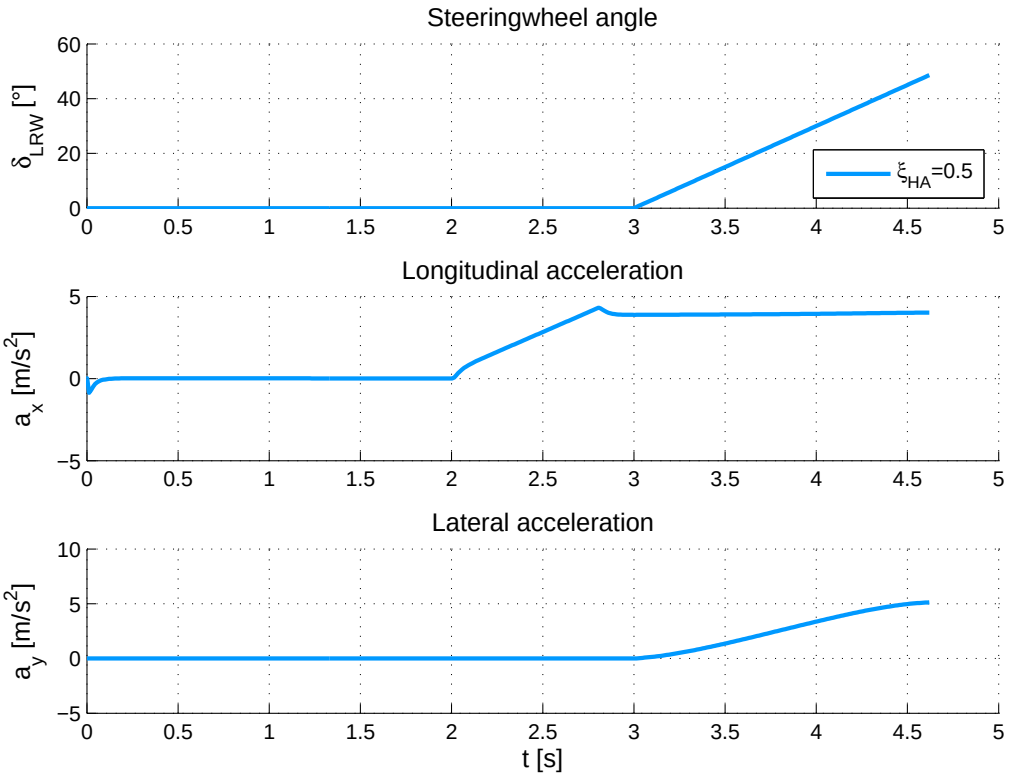

Figure 2.2: Overview of characteristic values of the maneuver used

linear region. This does not make the vehicle unstable at first. The real cause for instability is that the wheel reaches its saturation (κ limit) and thus cannot transmit more F_x. Another cause can be that the vehicle does not follow the driver's input anymore, and a_y changes more or less independent of δ_{LRW}. For example, for understeering behavior the vehicle does not react at the limit to further increase of the steering wheel angle, whilst for oversteering the driver has to adjust the steering wheel angle in opposite direction to decrease a_y and β. In (2.3) the stopping conditions are listed.

$$\begin{aligned} \beta &\geqq \frac{5}{180}\pi^\circ \\ \kappa &\geqq 10\% \\ |\delta_{LRW}| &\geqq 360^\circ \end{aligned} \tag{2.3}$$

2.3 Results

Here, first a basic understanding of the friction circle is provided. Then the results from the series of simulations performed to obtain the friction circle for different distributions ξ_{HA} are described and discussed.

In Figure 2.3 the friction circle is shown for different distributions. The friction circle shows the maximum lateral acceleration possible with respect to the longitudinal accelerations for a high friction coefficient $\mu = 1$. The maximum possible lateral acceleration is a measure for cornering performance because a high lateral acceleration means that the corner can be completed without becoming unstable at a higher speed:

$$\begin{aligned} a_y &= \frac{V^2}{R} \\ V &= \sqrt{a_y R} \end{aligned} \tag{2.4}$$

Looking at (2.4), it can be seen that when the radius R stays constant, a higher maximum possible lateral acceleration means that the speed with which the corner can be driven also increases. [1]

The simulations for this circle are performed with a high level of friction, $\mu = 1$. Similar investigations are performed on low friction levels of μ of 0.3, these are also discussed.

In Figure 2.3 the friction circle for this vehicle is shown. It becomes clear that changing the distribution can have a large effect on the cornering performance. The difference between best and worst distribution with regards to the maximum possible lateral acceleration is at some points more than $6\,\mathrm{m/s^2}$. This has implications for the safety of such a vehicle. Namely, when the limit is further away, the driver has more room for error since the maximum possible speed for that corner is higher. Because of the fact that the limit is further away, the behavior of the vehicle will be more predictable. This makes that a vehicle equipped with a system that optimally chooses the distribution is predicted to be safer than one with a fixed distribution.

Furthermore, the friction circle shows an increase in a_y at a slight deceleration (up until $-1\,\mathrm{m/s^2}$). This effect is caused by weight transfer. At a low negative a_x the front wheels will have more

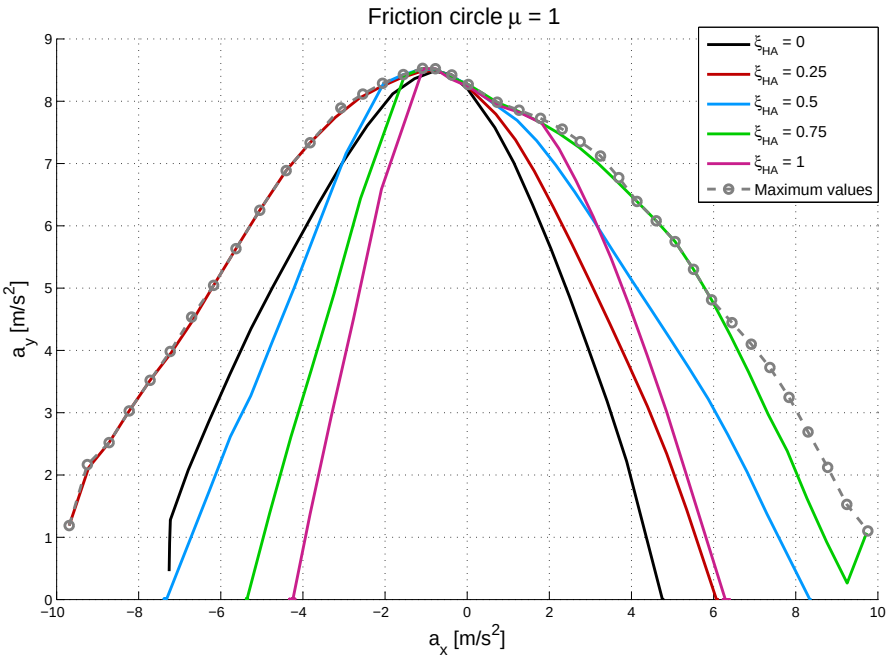

Figure 2.3: Maximum lateral acceleration versus longitudinal acceleration for different ξ_{HA} and the maximum values. Simulations performed with $\mu = 1$

potential due to increased F_z, meaning that a higher F_y can be transferred. This increases the maximum possible lateral acceleration. At a higher deceleration this effect is lost because κ is higher, which means that more of the tyre's total potential is used only to achieve the desired deceleration. The maximum lateral acceleration then decreases because there is less potential left for cornering.

Lastly, for a low $|a_x|$ it can be seen that there is not one distribution that reaches a significantly higher lateral acceleration within this range. This is shown in Figure 2.4, where the friction circle for $-1 \leq a_x \leq 1$ is plotted. For the lower longitudinal accelerations and decelerations it can be concluded that there is not one optimal distribution and it does not matter which distribution is used with regards to the maximum achievable lateral acceleration a_y. This was already expected since the longitudinal tyre forces are rather small and thus do not use a lot of the potential of the tyres. For a vehicle where ξ_{HA} can be controlled, this means that changing the distribution will only have an effect on the limit for higher longitudinal accelerations.

There is, however, one side note. Although the correct distribution can greatly increase cornering performance, care has to be taken that the *correct* distribution is chosen. The reason for this is that distributions exist that reach a higher a_y, but can lead to unstable or unpredictable behavior. These distributions eventually have too much longitudinal slip on the rear wheels. This can lead to oversteer [1], which is very difficult to control or react to for the average driver and thus unwanted. In that case, it is preferable to sacrifice some cornering performance in favor of safety. Namely, a slightly worse distribution in the sense of cornering performance can be safer because it eventually will have too much slip on the front wheels. This is a safer situation because it can lead to understeer, which is easier for an average driver to correct and predict and thus safer. In

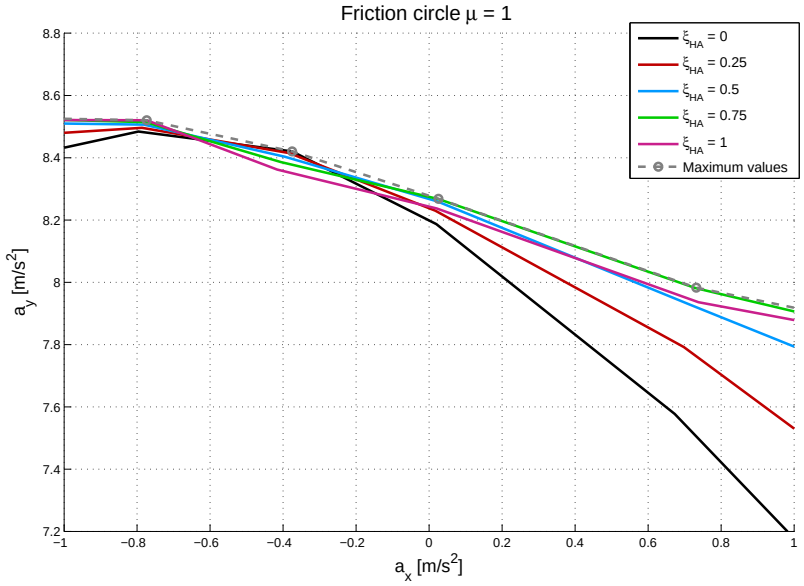

Figure 2.4: Friction circle for $-1 \leq a_x \leq 1$

conclusion, the distribution with the highest lateral acceleration with the best stability properties should be chosen. In Appendix A this is shown more in detail.

For a small friction coefficient $\mu = 0.3$ the same investigations are performed. In Figure 2.5 the friction circle for this low coefficient is plotted. The results are analogous to the high coefficient of friction. It appears that a weight distribution close to the stationary weight distribution gives highest cornering performance for accelerating. However, the same conclusions regarding to cornering performance and safety must be drawn for a low friction coefficient: at $\mu = 0.3$, it is also better to sacrifice some cornering performance in favor of predictability. For this situation this is especially true because the limit is much closer everywhere within the friction circle, as can be seen in Figure 2.5.

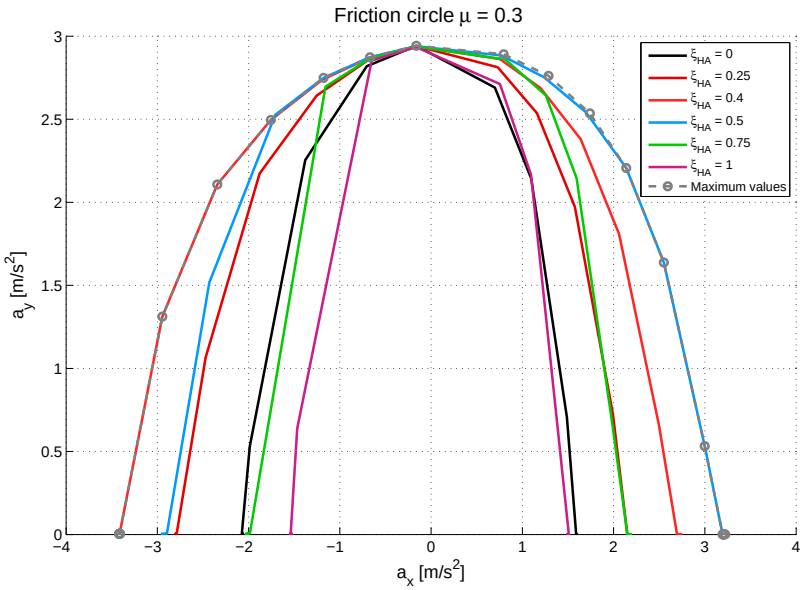

Figure 2.5: The friction circle with $\mu = 0.3$

2.4 Conclusion

The friction circle for different distributions ξ_{HA} is created by simulating driving in a circle with a certain longitudinal acceleration a_x and increasing steering wheel angle δ_{LRW} in order to obtain an increasing lateral acceleration. At the moment the vehicle becomes unstable (when κ or β is too high) the simulation is aborted. The point where the absolute value of the acceleration in both lateral and longitudinal direction is maximal is recorded. The total of these points form a friction circle for all the different distributions. This is done for two levels of friction, high ($\mu = 1$) as well as low ($\mu = 0.3$).

For a high coefficient of friction, the friction circle shows asymmetric behavior. For $|a_x| \leq 1\mathrm{m/s}^2$ there is not one single best distribution, the difference in cornering performance (maximal achieved lateral acceleration) is very small in that region. On the other hand, for higher values choosing the optimal distribution can mean a difference of more than $6\,\mathrm{m/s}^2$. The distributions with the highest a_y were about $\xi_{HA} = 0.25$ for braking and about $\xi_{HA} = 0.75$ for accelerating.

Some distributions reached a higher $a_{y_{max}}$. These distributions are more stable at a lower a_y since their limit is higher and further away. However, their drawback is that when the driver does use all of the available potential (approaches and/or reaches $a_{y_{max}}$) the vehicle becomes more difficult to handle and is less predictable. On the other hand, there are distributions that reach a slightly lower $a_{y_{max}}$ but do not have this drawback. The same goes for a low μ of 0.3. The tradeoff here is that the driver is given more room for error, but on the limit the driver might react wrongly because the vehicle can react unpredictably. As long as the reduction in maximum lateral acceleration is acceptable, it is preferable to have a slightly worse distribution with regards to lateral acceleration in favor of vehicle driveability and safety.

Chapter 3

Linear region

In Chapter 2 it was explained what happens on the friction limit for this vehicle, and what effects this has on the stability and driveability of the vehicle. Choosing the right distribution can increase cornering performance significantly while accelerating or decelerating, but care has to be taken that the distribution does not cause the vehicle to become undriveable at the friction limit or close to it. In general, it is preferable to choose a distribution with a slightly lower $a_{y_{max}}$ in favor of driveability and predictability of the vehicle. This, however, depends on how much cornering performance (and thus safety margin) one loses by that.

In this chapter, the linear region is further investigated. First, the maneuver that is used for this investigation is explained. The results are then discussed and a conclusion is drawn.

3.1 Introduction

To recapitulate, in Figure 3.1 the regions of interest are shown again.

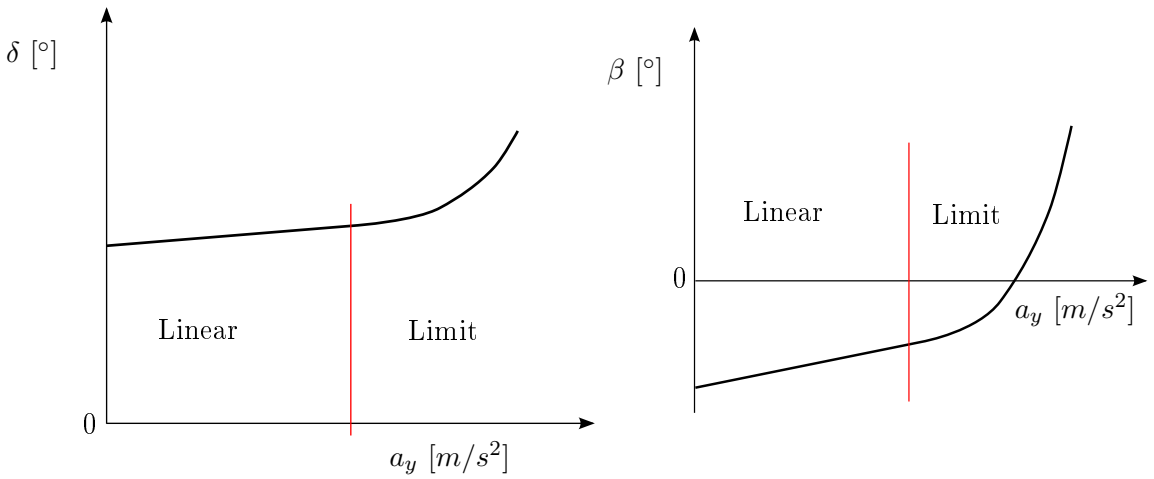

(a) Steering wheel angle δ versus lateral acceleration a_y

(b) Vehicle side slip angle β versus a_y

Figure 3.1: Overview of the two regions of interest

The linear region is characterized by a linear relationship between the lateral acceleration and the required steering wheel angle, and between the lateral acceleration and the vehicle side slip angle. This can be seen in Figure 3.1. In the previous chapter the limit region was discussed. This region was characterized by a (highly) non-linear relation between the lateral acceleration and the

steering wheel angle and the vehicle side slip angle. In contrast to the limit region, the linear region is investigated under low lateral accelerations and side slip angles. The linear region is in principle independent of the longitudinal acceleration. However, the region where the linear region is given and/or valid is influenced by the longitudinal acceleration. As seen in the previous chapter, a higher a_x causes the vehicle to reach the limit (and thus enter the non-linear behavior) earlier.

Of interest here is the self steering behavior of the vehicle, and to what degree that changes with respect to a changing distribution. This shows what influence the distribution has on the driving behavior of the vehicle in a quasi steady-state cornering situation. Usually, this is evaluated without longitudinal acceleration. Here, however, the term linear region means that the longitudinal accelerations are low ($|a_x| \leq 2\,\mathrm{m/s^2}$).

The self steering behavior of the vehicle is mainly characterized by two values. Firstly, it is characterized by the degree to which the steering wheel angle needs to be adjusted with an increasing lateral acceleration. The driver has to steer less or more when the lateral acceleration increases. This is the understeer gradient (abbreviated EG). The other parameter that is of interest is the vehicle side slip angle gradient (abbreviated SG). The SG describes the degree to which the vehicle side slip angle increases or decreases with an increasing lateral acceleration. The EG and SG are defined as:

$$\begin{aligned} EG &= \frac{\partial \delta_{LRW}}{\partial a_y} \cdot \frac{1}{i_L}\,[^\circ/(\mathrm{m}\cdot\mathrm{s}^2)] \\ SG &= \frac{\partial \beta}{\partial a_y}\,[^\circ/(\mathrm{m}\cdot\mathrm{s}^2)] \end{aligned} \tag{3.1}$$

Here, δ_{LRW} stands for the steering wheel angle in degrees, i_L is the ratio from steering wheel angle to the steering angle of the front wheels. In this case, it is presumed to be a constant. Generally, the steering ratio is not a constant but changes with rack displacement and due to (elasto-)kinematics on the front wheels.

Now, the maneuver that is used for the investigation of the linear region is explained.

3.2 Used maneuver

The maneuver that is used here is quite similar to the maneuver used as described in Chapter 2. The difference is, however, is that the steering wheel angle is controlled in such a way that the radius remains constant. The required steering wheel angle (δ_{LRW}) is then recorded, as well as the vehicle side slip angle β and together with the achieved lateral acceleration. These maneuvers are also performed for several distributions. In Figure 3.2 the characteristic values for this maneuver are shown. The steering wheel angle and both lateral and longitudinal acceleration are plotted in time. This particular figure was generated with a distribution of exactly 50%.

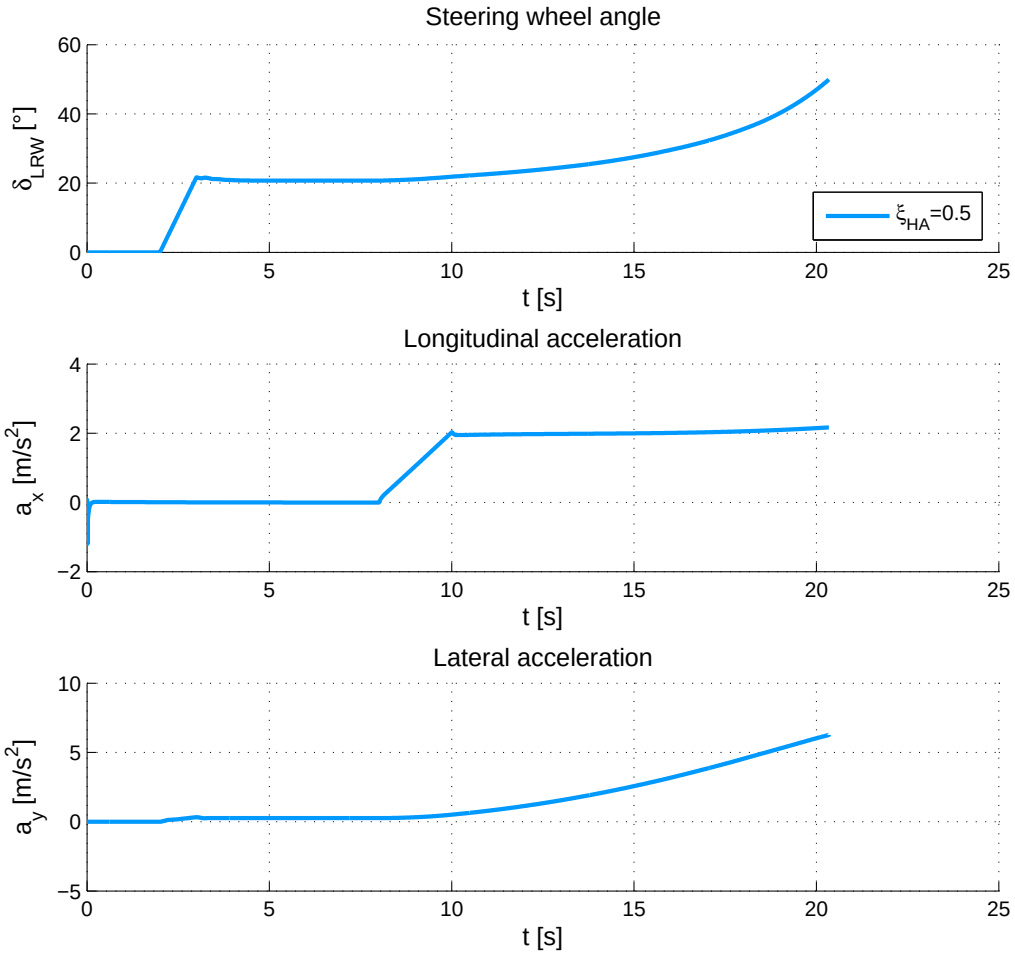

Figure 3.2: The characteristic values for this maneuver in time

As can be seen, at around 3 seconds the steering wheel angle is gradually increased in order to make the vehicle drive on a constant radius. Further on a steering controller assures that the vehicle turns on a constant radius. At about 8 seconds the longitudinal acceleration is increased linearly to the target value, which is $2\,\mathrm{m/s^2}$ in this case. Thus, with the rising velocity also the lateral acceleration is increased. The maneuver is performed until the transition to the non-linear vehicle behavior is observed. For a small a_x the stationary behavior can be investigated. The reason for this is that it is necessary as a reference to show how the vehicle behaves for no acceleration, but it is not possible to perform a simulation where the longitudinal acceleration is zero. Therefore, a low acceleration is chosen to approximate this. The results from this maneuver then represent the non-accelerated stationary cornering behavior. For higher a_x the quasi-stationary behavior under certain longitudinal accelerations can be observed. The same stopping conditions apply as discussed in Chapter 2.

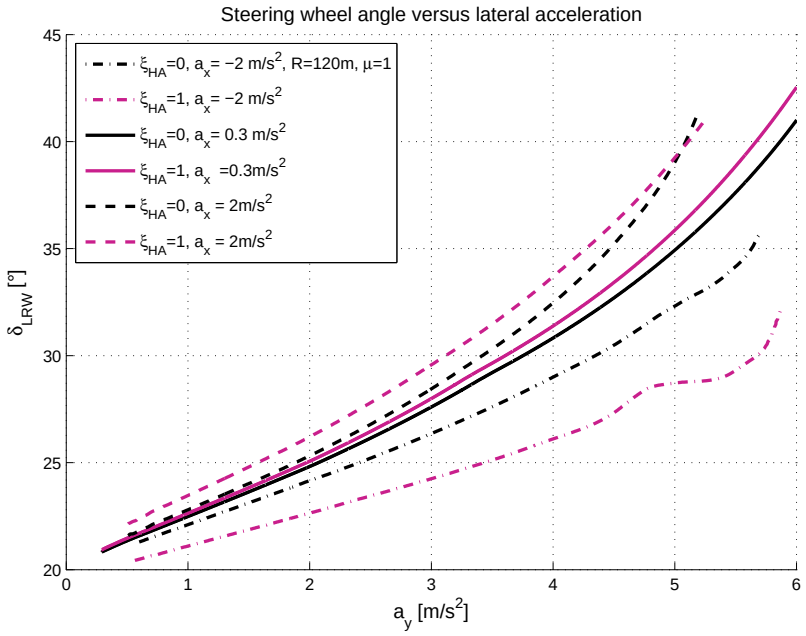

Figure 3.3: Steering wheel angle versus lateral acceleration for 3 different longitudinal accelerations and $\xi_{HA} = 0$ and 1

3.3 Results

In Figure 3.3 and Figure 3.4 the steering wheel angle and vehicle side slip angle versus the lateral acceleration are plotted. In both figures two distributions are plotted, namely for fully front wheel driven and fully rear wheel driven. All simulations are performed on a road with a high coefficient of friction $\mu = 1$. The corner radius was controlled at $R = 120\,\mathrm{m}$. The simulations that are performed are for longitudinal accelerations of $-2\,\mathrm{m/s^2}$, $0.3\,\mathrm{m/s^2}$ and $2\,\mathrm{m/s^2}$. The simulation where $a_x = 0.3\,\mathrm{m/s^2}$ represents the reference curve for the non-accelerated stationary cornering behavior.

As mentioned earlier in Section (3.1), the EG and SG are defined as the gradient in the linear region of the steering wheel angle and vehicle side slip angle. These parameters are plotted in the above graphs. From this, it becomes clear that there is not much potential for a variable torque distributing system within the linear region. Between the distributions, there is little difference in steepness of the figures (the EG and SG). These characteristic vehicle parameters can therefore not be (strongly) influenced by a variable distribution.

In Figure 3.3 and 3.4 a greater difference in EG and SG can be seen between the different distributions for decelerating than accelerating. The reason for this is that the cornering stiffness changes more for negative longitudinal slip than for positive. Apparently the tyres degrade faster when applying negative slip. This leads to a faster increase or decrease in EG and SG because then the tyres are more inclined to lose grip. This explains the behavior for the difference in EG and SG with respect to the longitudinal acceleration. For a more detailed investigation, see Appendix B.

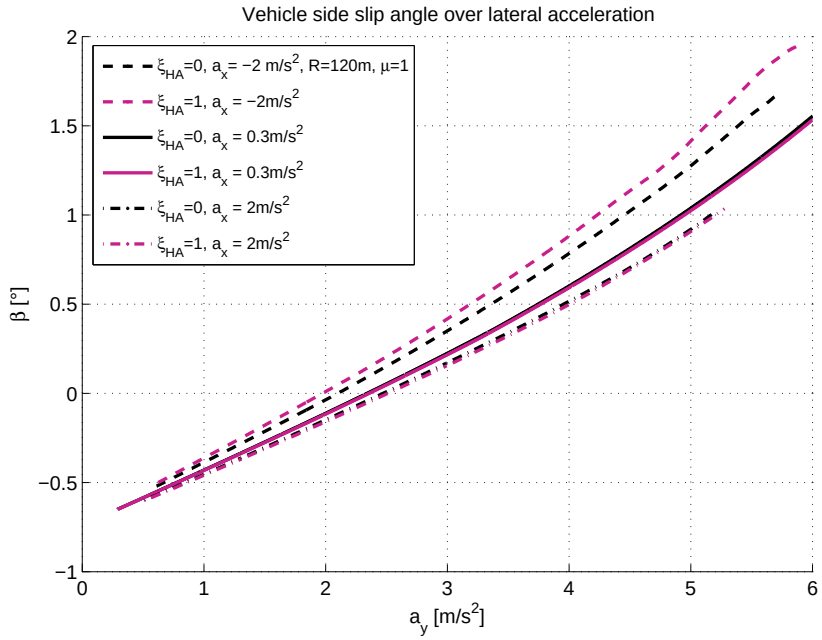

Figure 3.4: Vehicle side slip angle versus lateral acceleration for 3 different longitudinal accelerations and $\xi_{HA} = 0$ and 1

3.4 Conclusion

In this chapter the linear region is investigated. The region is investigated with low longitudinal accelerations and almost zero a_x. The near zero longitudinal acceleration is necessary as an approximated reference for the non-accelerated almost stationary behavior. It appeared that for a low (but not near zero) $|a_x|$ the distribution does not make a big difference, especially with respect to the understeer gradient EG and vehicle side slip gradient SG. The main difference is in the amount of Ackermann steering needed, which is characterized by the constant offset of the steering wheel angle in a $\delta - a_y$ graph. This is because of kinematic and elastokinematic effects in the suspension and steering system. For a negative a_x there is more difference in EG and SG between the different distributions than for a positive a_x. Further investigations have shown that the reason for this appears to be the asymmetric tyre behavior. The change in cornering stiffness is higher for a negative longitudinal slip κ than for a positive κ. This leads to changes in the understeer gradient and side slip gradient.

In the following chapter the design of the controller will be explained. This chapter explicates what the goal of the controller is, the design and testing of the controller and finally the results.

Chapter 4

Controller design

In previous chapters the limit region and the linear region are discussed. It appears that in the limit region the distribution ξ_{HA} has a positive influence on the behavior of the vehicle and the driveability, especially on the limit. In the linear region ξ_{HA} has less influence on the selfsteering behavior of the vehicle (described by the vehicle side slip gradient and understeer gradient). Furthermore, it appears that there is more change in EG and SG when braking than for accelerating. This is caused by the tyre model, which shows asymmetrical behavior in the F_x and F_y axis.

In this chapter, it is explained what the objective of the controller is and how it is set up. Furthermore, the tests of the controller are described and the results thereof. Finally, some improvements are formulated.

4.1 Controller objective

Here, a vehicle where the torque distribution between the axles can be changed is investigated. The controller controls the distribution ξ_{HA}. The aim is to create a controller that stabilizes the vehicle, and makes optimally uses the tyres. Ideally, the controller chooses the correct distribution in every situation it encouners. This can be done in several ways. Firstly, one could think of a feedforward controller that measures both the longitudinal and lateral acceleration, and based on previous investigations chooses the corresponding best distribution. Another option is also a feedforward controller, but one that calculates the potential that is left on the wheels and distributes the driving or braking torque accordingly. This option was also created and tested in the driving simulator, but this will not be elaborated here. A feedback controller is another possibility. This is the controller that is described here.

It is decided to control the yaw rate of the car. The reference yaw rate is not one of an artificial model, but it is derived from the steady state cornering vehicle. As has been seen in previous chapters the steady state yaw rate for $a_x = 0$ is almost independent of the distribution ξ_{HA}, because in this case there are almost no drive forces applied to the vehicle. When the yaw rate with respect to the reference becomes too high, it means that the vehicle is steering more than it should be. Hence, it is heading to an oversteering behavior. Vice versa, when the measured yaw rate is lower than the reference, the understeering behavior increases. This behavior will be corrected by the controller via ξ_{HA} in such a way that the car is driving the reference yaw rate as much as possible.

4.2 Controller design

The reference for the controller is the steady state yaw rate of the vehicle ($\dot{\psi}_{ref}$). This steady state value is compared with the actual measured yaw rate of the vehicle ($\dot{\psi}$). The error, the difference between the two yaw rates, should be reduced by changing ξ_{HA} accordingly. The error is as follows:

$$\dot{\psi}_{ref} = \frac{1}{i_L} \cdot \frac{v_x}{L + EG \cdot v_x^2} \cdot \delta_{LRW} \tag{4.1}$$

$$e = \dot{\psi} - \dot{\psi}_{ref} \tag{4.2}$$

This is actually an approximation of the yaw rate, since it uses an approximation for the wheel steering angle. The approximation between wheel steering angles and steering wheel angle is an approximation because the gear ratio of the rack/pinion steering gear is not constant with displacement, the kinematic of the steered wheel is different for left or right turns and left and right side. Furthermore, the elastokinematic steering is dependent on the current force state at the wheel. The wheel steering angle δ_s is therefore approximated by taking the steering wheel angle δ_{LRW} as an input. This is related by (2.2). However, i_L is not a constant factor, and the resulting δ_s is therefore an approximation. In practice however, this proved good enough. This parameter, along with the EG and L are obtained from the parametrization and steady state simulations of the non-linear full vehicle model.

The output is described as follows:

$$\begin{aligned} \xi_{HA} &= \xi_{PI} + \xi c \\ &= Pe_t + I \int e_t \, \mathrm{d}t + \xi_c \end{aligned} \tag{4.3}$$

Here, ξ_c is a constant distribution which represents the default value when no dynamical control is acting. This value is, for example, set by the powertrain strategy. The most stable compromise for both low and high friction levels ($\mu = 1$ and $\mu = 0.3$) and braking and accelerating proved to be about 0.5. Therefore, the initial distribution here was set to this value. With $\xi_c = 0.5$, the vehicle starts at a 50% distribution. An added benefit of this is that it takes a shorter time to reach both $\xi = 1$ and $\xi = 0$ than it would if the output would start at 1 or 0.

The output ξ_{HA} is finally saturated between 0 and 1 because it cannot be any lower or higher than these limits. In Figure 4.1 a block diagram of the controller is given.

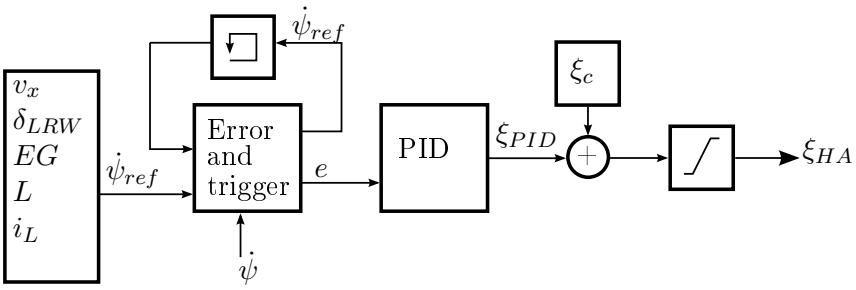

Figure 4.1: Schematic overview of the strategy to obtain the friction circle for one distribution

4.3 Simulation and test results

The controller is tested in the driving simulator with real drivers and also tested using simulated maneuvers similar to the ones used to create the friction circle.

4.3.1 Test in driving simulator

Both the wheel potential controller and the yaw rate controller were tested in the driving simulator. The simulator was set up for driving in a circle with a radius of around 200m. The coefficient of friction of the road was set to low, $\mu = 0.3$

The test subjects were first shown a car with constant distributions from 0 to 1, and told to drive, accelerate and brake in the corner. On this surface, the distributions of 0 and 1 proved to be most difficult to drive. This was already predicted in Chapter 2. When the distribution was set close to the stationary weight distribution of the vehicle, which is around 50%, the vehicle felt the most stable. However, when braking, it appeared that the vehicle became unstable too early, or showed strong oversteering behavior. The common setup for current all-wheel drive vehicles is one where braking is done with $\xi_{HA} = 0.35$ and driving with $\xi_{HA} = 0.55$. It was therefore suggested to test a distribution with this setup as the benchmark variant. This setup was tested and proved to be more stable when braking and showed less oversteering behavior when braking.

Using the constant distribution as a reference, the vehicle was then tested with a variable distribution. There were two different controllers tested. One was a feedforward controller using the leftover wheelpotential to optimally distribute the driving forces, and the other was the aforementioned yaw rate controller. The latter PI controller is of interest here.

Again, drivers were asked to drive, brake and accelerate in the corner. When given the variable controlled distribution, the drivers reported a significant improvement in handling, compared to the cars with a constant distribution. The subjective impression was that the car was more stable and that more lateral acceleration could be reached than with a constant distribution. Moreover, when the drivers braked in the corner, the driven radius was almost constant. This means that there were no steering corrections necessary to keep the car on track. Due to the reduced steering effort and the increased safety feeling of the driver, a vehicle equipped with such a controller is safer than without since the danger of wrong or too big or too small driver interventions is reduced.

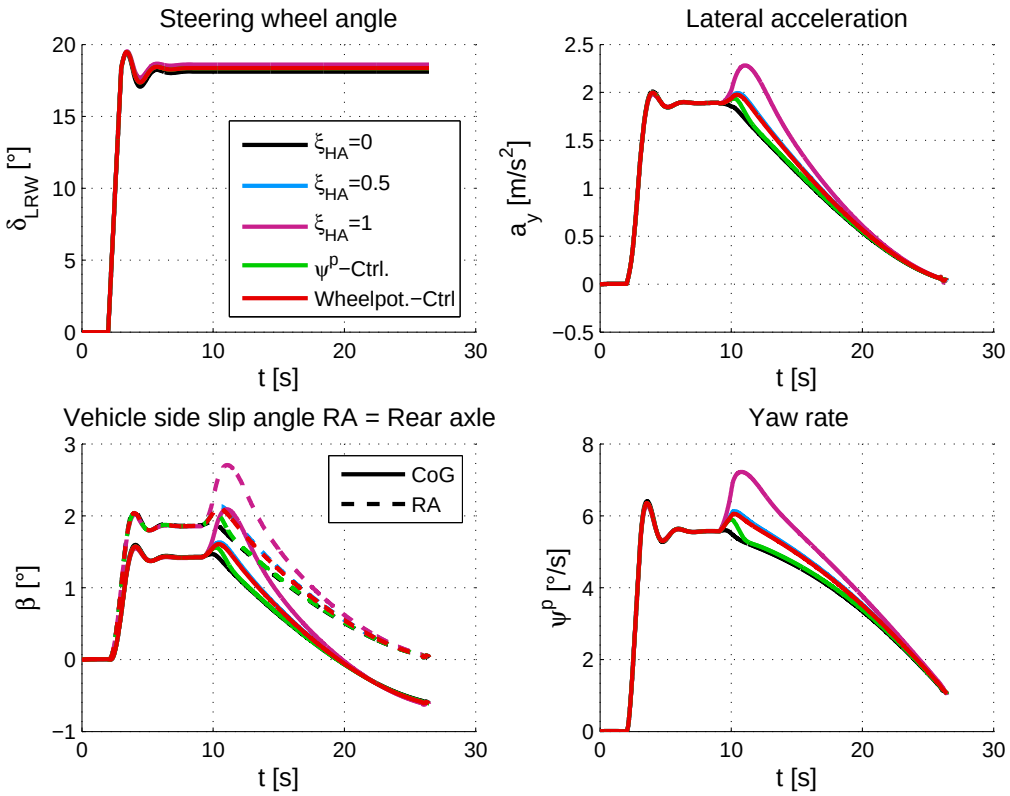

Figure 4.2: Cornering parameters for three constant distributions and two controllers

4.3.2 Simulations

Using the EG as calculated in the previous subsection, the controller is also tested in a virtual environment. The subjective results that were collected during testing in the driving simulator were confirmed here. In these simulations, in the beginning the radius is kept constant, but after around 5 seconds the steering wheel angle is kept constant. This can be seen in Figure 4.2.

In Figure 4.2 the steering wheel angle, lateral acceleration, vehicle side slip angle and yaw rate in time are displayed. These values are shown for five different systems: a front wheel driven car, an all wheel driven car with $\xi_{HA} = 0.5$, a rear wheel driven car. Furthermore, two controllers are displayed: the yaw rate controller and wheel potential controller. The gains were previously experimentally determined in the driving simulator. It can be seen that for a constant steering wheel angle the rear wheel driven vehicle the yaw rate shows a peak, while the front wheel driven vehicle elicits a more stable response. In between these two the yaw rate controller can be found. The controller appears to dampen the initial peak, and then controls towards $\xi_{HA} = 0$. This can be seen from the fact that the yaw rate controller shows the same behavior as the front wheel driven vehicle. The lowest yaw rate is that of the front wheel driven car, and that is where the controller tries to control to.

For the driven radius, shown in Figure 4.3, this corrective action can also be seen. For this figure, the same braking maneuver with a constant steering wheel angle is driven. The radius of the

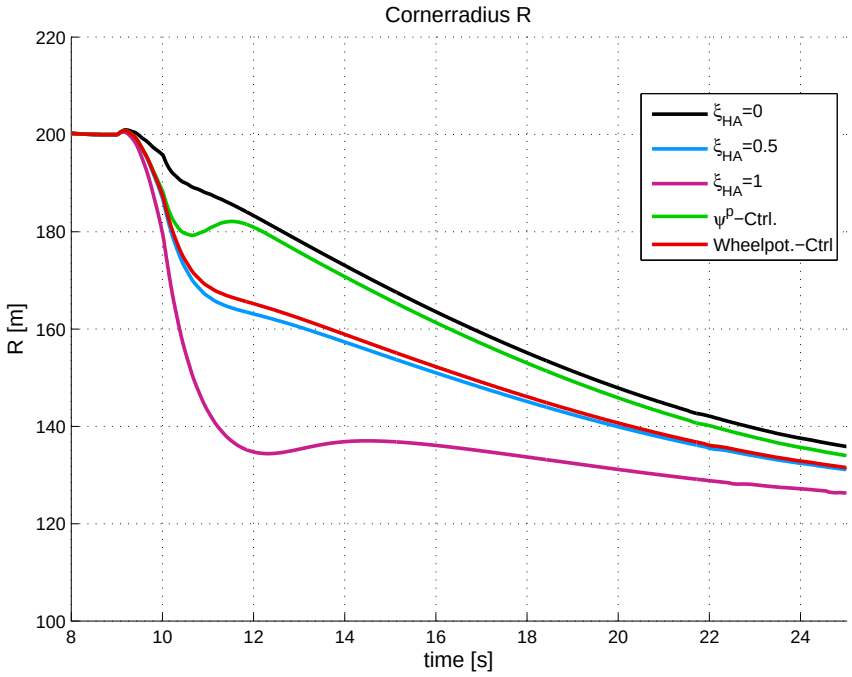

Figure 4.3: Driven radius for three constant distributions and two controllers

vehicle is here displayed.

It is assumed that the driver wants to corner with an as constant radius as possible. This means that a large deviation in the driven radius is undesirable. The reason for this is that the driver in that case would have to make severe corrections in the vehicle driving behavior, which could lead to an unstable vehicle. Moreover, such corrections can be very difficult to handle for the average driver. In the figure above it becomes clears that then a vehicle with $\xi_{HA} = 1$ is the least desirable for this maneuver. In this case, the braking was done on the rear wheels only. A vehicle where $\xi_{HA} = 0$ shows the most stable decline in driven radius. The controlled vehicle (green line) has an initial drop in driven radius (however not as large as $\xi_{HA} = 1$, but corrects quickly and moves towards $\xi_{HA} = 0$ and declines steadily. Since the vehicle cannot move past $\xi_{HA} = 0$, this is in this case the most desirable behavior.

The advantage of such a control system is that the distribution can be adjusted online. In this example a front wheel driven car appears to be the ideal distribution, but there are of course other situations where a rear wheel driven vehicle is ideal. Moreover, in low friction situations a vehicle with a more 50/50 distribution performed best. This is already shown in previous chapters. In short, different situations require different distributions. With a controlled torque distribution, the best distribution in every situation can be approximated online, thus adapting to the different situations. This is of course impossible for vehicles with a fixed distribution. Therefore, a vehicle with a variable distribution will be beneficial for the driving behavior. It dynamically improves stability and predictability by maintaining an as steady as possible yaw rate in every situation the vehicle encounters.

4.4 Conclusion

In this chapter, a PI yaw rate controller was developed to control the longitudinal force distribution ξ_{HA}. This controller consists of a PI controlled part and a constant distribution. The total controller (together with a wheel potential controller that is not discussed in this document) is tested in a virtual environment and in a driving simulator with human test subjects. In the driving simulator the test subjects drove in a constant corner with a radius of around 200 meters and a friction coefficient $\mu = 0.3$. This maneuver is driven because of restrictions in the simulator. The drivers reported a much more stable car which is able to reach a higher lateral acceleration when braking or acceleration. Furthermore, when accelerating or braking in the corner there was not as much steering correction necessary to keep the car on the desired radius. The simulated results confirm this behavior and show that this yaw rate controller is beneficial to the driving behavior of a car on surfaces with a low friction, and making it able to adapt to different situations.

Chapter 5

Conclusion and recommendations

In previous chapters the limit region and linear region was investigated. Furthermore, a controller was designed and tested. In this chapter conclusions are drawn based on previous investigations and recommendations are made.

5.1 Conclusions

In this report a vehicle that can distribute the drive or brake torque freely between its front and rear axle is investigated (distribution percentage is called ξ_{HA}). The behavior of such a vehicle on the friction limit and in the linear region is of special interest. Furthermore, the scope of this research is limited to regions where both axles are either driving or braking; situations where one axle is operating in an opposite direction with respect to the other axle are neglected. The results are obtained using a full vehicle model simulation that drives two different maneuvers. For the limit region the steering wheel angle is gradually increased until instability, and for the linear region the radius is controlled. At both maneuvers a longitudinal acceleration is applied additionally.

For the limit region it appears that the distribution has a large positive influence on the maximum achievable lateral acceleration. Choosing the right distribution could mean a difference up to $6\,\mathrm{m/s^2}$ on a road with a high coefficient of friction. For a low friction coefficient $\mu = 0.3$, the difference is lower but the results are comparable. All distributions eventually become unstable with the maneuvers used to investigate the friction circle. There are, however, differences in the behavior at the limit. Some distributions lead to oversteering behavior, whilst some lead to understeering behavior. Since understeering behavior is easier to handle for the average driver, these distributions are considered to be safer. It appears that while some distributions have a lower limit, i.e. these distributions reach a lower maximum lateral acceleration before becoming unstable, they are easier to handle for the driver because their instability leads to understeering behavior. It is therefore concluded that a lower limit in favor of driveability and predictability is preferred, as long as the reduction in $a_{y_{max}}$ is acceptable.

The linear region can be less influenced by the distribution. For lower accelerations and decelerations the difference in under steer gradient and vehicle sideslip gradient between the distributions is low. However, the difference between EG and SG is higher for braking situations than for accelerating. This is due to a tyre asymmetry, because the cornering stiffness changes more for negative κ then for positive κ. This influences the two gradients.

Finally, a PI controller is created that controls the yaw rate. This controller is tested in both a driving simulator and using offline simulations. The test subjects in the driving simulator reported a significant increase in driveability of the car. This result is confirmed in the virtual

environment. The steering effort from the driver was reduced significantly and the vehicle was easier to control for the driver, especially since oversteering behavior could be reduced.

The conclusion can therefore be drawn that a system that controls the distribution ξ_{HA} has potential, mainly because the vehicle drives more predictable and requires less steering effort when braking or accelerating in a corner. Furthermore, it can react to changing circumstances better than a car with a fixed distribution. Take for example a situation where the driver exits a highway. Here, a steady deceleration in a corner with constant radius R is required. If there is a patch of ice on this road and desired radius, the vehicle that is equipped with a yaw rate ξ_{HA} control could react to this patch of ice by distributing more towards 50%. This increases stability of the vehicle, and makes sure the driver stays on the road. Moreover, the driver does not need to suddenly steer more or less to keep the corner because the controller is able to steer the vehicle in he required radius. There is, however, one side note to be made. Namely, when a vehicle is equipped with ESP the braking interventions are mainly responsible for maintaining cornering stability. The yaw rate controller for a variable distribution vehicle can get the vehicle as stable as possible, after which the ESP does not need as much stabilizing effort as in a vehicle without such a controller. Furthermore, in this investigation, mainly quasi-stationary maneuvers are investigated. However, there is also potential for such a system in non-stationary maneuvers.

5.2 Recommendations

There are, however, some improvements possible. The reference model for the controller, which is currently a simple steady state model, needs to be improved. Furthermore, the constant steady-state distribution ξ_c that is added behind the PI controller is now constantly set to 0.5. This starting factor will eventually be dependent on the powertrain strategy (fuel saving, battery charging, etc.). This will give the initial value. This is also the reason why the controller should not operate in the low longitudinal acceleration region, in order to not disturb the powertrain strategy in regions where the vehicle dynamics can anyway only be slightly influenced. For further research, it should be investigated if different starting values would cause any significant change in the beginning. For a properly working controller the final value should be the same.

Appendix A

Analysis of friction circle

Here, a more elaborate analysis of the friction circle for this vehicle will be provided. This is done for both a large friction coefficient, as well as a small. Furthermore, it is investigated what effect the changing distribution has on the stability, safety and predictability of the vehicle on the limit.

A.1 Large μ

To illustrate the effect of being able to change the distribution, first suppose that a vehicle does not have a variable torque distribution, but only front wheel drive. The friction circle corresponding to that is shown in Figure A.1a. The total range of operation with regard to the longitudinal acceleration of such a vehicle is between $-7\,\mathrm{m/s^2}$ to $5\,\mathrm{m/s^2}$. For values outside this range, the possible lateral acceleration is zero. Please note that within these simulations, braking is done according to the distribution. That means that in this case, braking is also done completely on the front wheels. The reason for this is that the potential of regenerative braking is also of interest and therefore has to be included in the simulations. This is not possible if a conventional braking system is applied, as this will of course lead to different results in the negative a_x region.

Now, consider a vehicle that has a distribution that can be switched from front wheel drive to rear wheel drive, so ξ_{HA} is either 0 or 1. This vehicle's friction circle is shown in Figure A.1b. Now, the range of operation is extended to $-7 \leq a_x \leq 6\ \mathrm{m/s^2}$ by being able to switch between the two distributions. Moreover, the cornering performance is increased substantially if the vehicle can switch between these distributions. For example, with a longitudinal acceleration of $4\,\mathrm{m/s^2}$ the maximum possible lateral acceleration is increased from around $2\,\mathrm{m/s^2}$ for the front wheel driven vehicle to around $5\,\mathrm{m/s^2}$ for the vehicle that can switch between the two distributions. This means that even a basic changing distribution can be beneficial for the cornering performance, since the total friction circle is wider, meaning that the vehicle has a broader range of operation.

For the total friction circle with all distributions this conclusion remains the same. In Figure A.2 the total friction circle is shown. A vertical line at $-4\,\mathrm{m/s^2}$ is added to indicate the difference in maximum lateral acceleration between the different distributions at that a_x.

It is already explained that the difference between different distributions can be significant with respect to the maximum achievable lateral acceleration. The same can be seen here, where the total friction circle is plotted, including the maximum achieved values. The difference between the best and worst distribution at the vertical red line ($a_x = -4\,\mathrm{m/s^2}$) is the difference between $a_y = 1\,\mathrm{m/s^2}$ for $\xi_{HA} = 1$ and $a_y > 7\,\mathrm{m/s^2}$ for $\xi_{HA} = 0.25$. This means that in this case, choosing the right distribution can mean a difference in maximum possible lateral acceleration of more than $6\,\mathrm{m/s^2}$. The same goes for positive a_x. In general, the conclusion can thus be drawn that for the cornering performance, choosing the right distribution is crucial. In this case, the

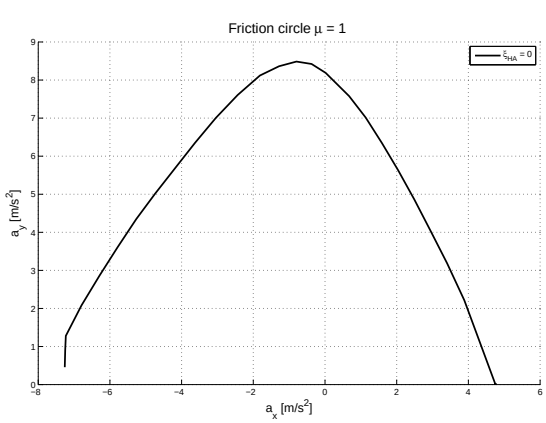

(a) Friction circle for a front wheel driven car

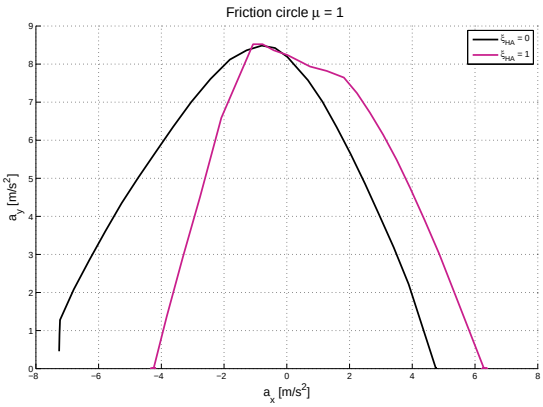

(b) Friction circle for both a front and rear wheel driven car

Figure A.1: Friction circle

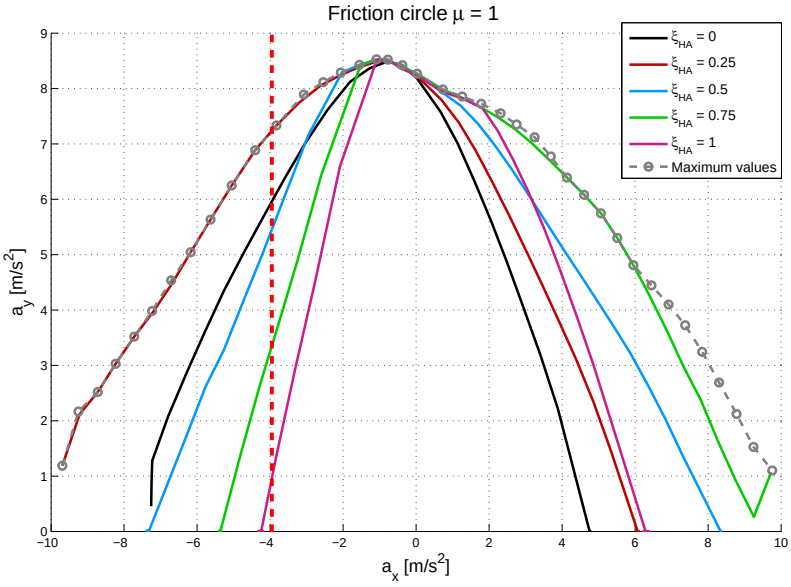

Figure A.2: Friction circle for $\mu = 1$

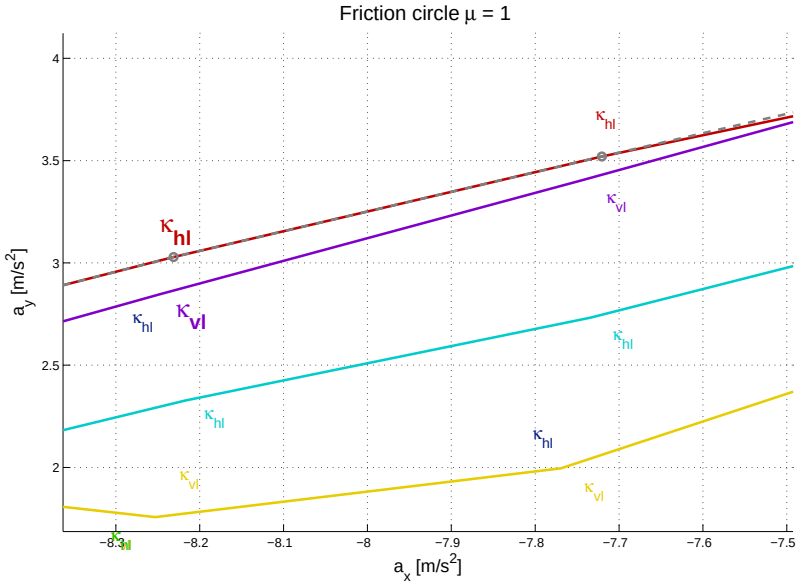

Figure A.3: Friction circle zoomed in with markers that indicate stopping condition

best distribution is about 25% when braking and about 75% when accelerating. There are better variants that are not explicitly plotted (for readability's sake), but can be concluded from the grey 'Maximum values' line.

Furthermore, the reason why simulations are stopped should be taken into consideration. In Figure A.3 the friction circle for $\mu = 1$ is again plotted, together with markers which indicate the reason why the simulation is stopped. In this case, κ means that the longitudinal slip was too high (greater than 10%). The subscript indicates the wheel, where v means front wheel, h means a rear wheel. Moreover, l stands for a left wheel, while r means a rear wheel. So, here κ_{vl} means the slip on the front left wheel becomes too high, and κ_{hl} indicates that the slip on the rear left wheel is greater than 10%. Since a too high slip on the rear wheels can lead to oversteer, it is preferable to choose a distribution that ultimately aborts because of a too high slip on the front wheels (which can lead to understeer). Namely, oversteer is much harder to correct and predict for the average driver than understeer and is therefore more unsafe.

A.2 Small μ

In the previous section the friction circle for a higher coefficient of friction was investigated. Here, the same is done, but for a lower coefficient of friction. These simulations are performed with a coefficient of friction $\mu = 0.3$. This can be compared with driving on snow and ice with normal tyres. The maximal possible accelerations are therefore a lot smaller in both longitudinal and lateral direction, since $F_s \leq \mu F_z$ [1].

In Figure A.4 the friction circle for this low coefficient is plotted. As expected, both a_x and a_y are lower than is the case for the higher coefficient of friction. The maximum lateral acceleration is around $3\,\mathrm{m/s^2}$, whilst for the high μ it reaches around $8.5\,\mathrm{m/s^2}$. It appears that the line for

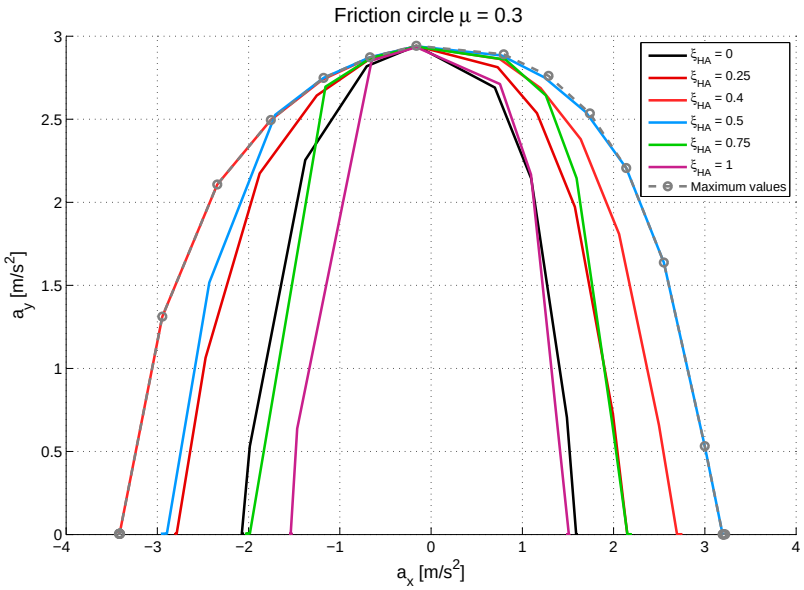

Figure A.4: The friction circle with $\mu = 0.3$

the maximum values coincides with $\xi_{HA} = 0.4$ for negative a_x, and almost completely coincides with $\xi_{HA} = 0.5$ for acceleration. For a low coefficient of friction, so for bad road conditions, it is favorable to distribute the driving and braking torque more evenly and close to the stationary weight distribution of the vehicle. The influence of the longitudinal weight transfer is quite small since the longitudinal acceleration is rather low.

Looking more closely at the area between 1.2 and 2 $\mathrm{m/s^2}$, as shown in Figure A.5, it is visible that the distribution of 60% can reach a higher lateral acceleration. Here, the friction circle for $\mu = 0.3$ is plotted for previously mentioned range together with the markers that indicate the stopping condition. The meaning of κ is already explained. β indicates that the vehicle side slip angle β is greater than 5°. From Figure A.5, it is visible that for $\xi_{HA} = 0.6$ the vehicle reaches a side slip angle that is too high. This means that the tyres are saturated not in the longitudinal direction (as is the case when κ is too high), but in the lateral direction. The rear wheels cannot transmit more F_y, thus increasing the vehicle side slip angle. What is stated for the higher coefficient is therefore also applicable here: the best distribution is the one with the highest lateral acceleration and stability properties, especially since the difference in maximum achievable lateral acceleration is quite small.

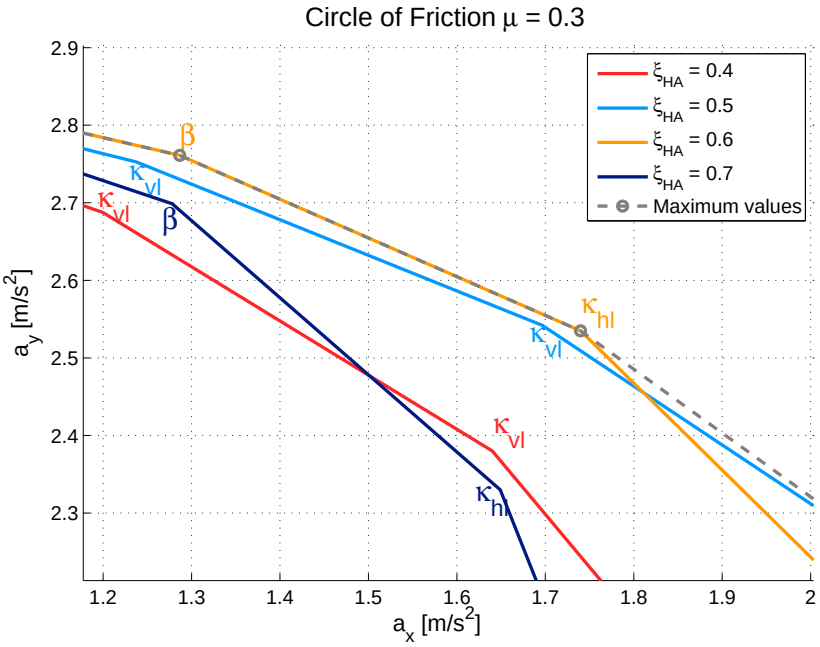

Figure A.5: The friction circle with $\mu = 0.3$ zoomed in and markers added

Appendix B

Investigation of change in gradients

Here, it is investigated why the understeer gradient (EG) and vehicle sideslip gradient (SG) change more for a negative longitudinal slip than it does for a positive longitudinal slip. This effect is shown in Figure B.1 and B.2. To further investigate this, in Figure B.3a and Figure B.3b several distributions are plotted for a_x of $-2\,\mathrm{m/s^2}$ and $2\,\mathrm{m/s^2}$.

It is clear that the gradient difference between the different distributions is very small. This applies to both accelerating and decelerating. However, the difference in EG is greater for negative a_x than for positive a_x. The biggest difference is the constant offset of the steering wheel angle, which is Ackermann steering.

In Figure B.4 EG is shown versus the longitudinal acceleration for three different distributions, namely $\xi_{HA} = 0, 0.5$ and 1. From this figure it becomes clear that the difference in under steer gradient is greater for negative a_x than for positive a_x. The reason for this can be found in the model used for the tyres. The combined force states of the used tyres are shown in Figure B.5. Here, the longitudinal and lateral force of the tyre used is plotted with κ and α iso-lines. As can be seen, this globe is not symmetrical in the F_y axis and F_x axis.

For negative F_x it appears to bend stronger on the outer edges than for positive F_x. This behavior is confirmed when looking at Figure B.6. This Figure shows different stiffnesses and their percentual change with respect to the longitudinal slip and sideslip angle. Here, it becomes clear that the change in cornering stiffness with respect to longitudinal slip is greater for negative κ. Apparently the tyres lose grip faster for negative slip than for positive slip (this can also be seen in Figure B.5). Because of this, the EG and SG change more in the negative κ region.

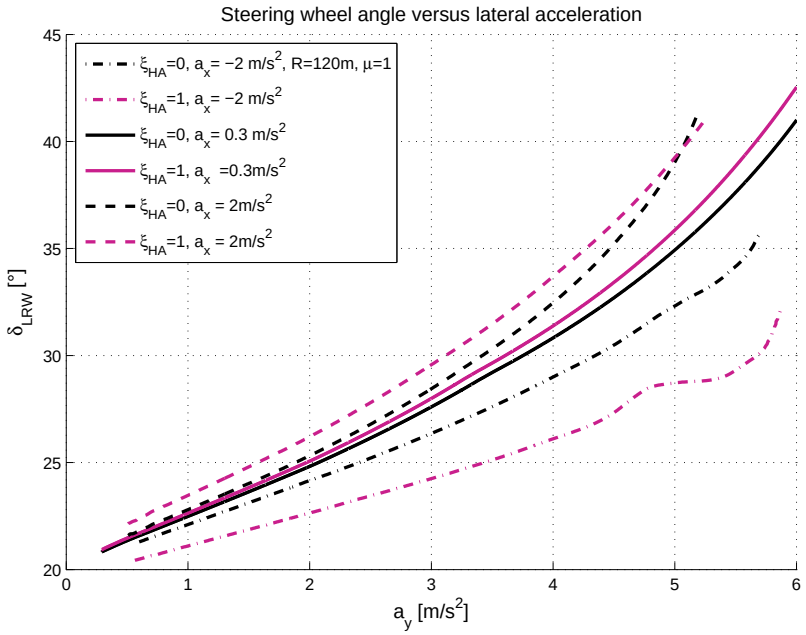

Figure B.1: Steering wheel angle versus lateral acceleration for 3 different longitudinal accelerations and $\xi_{HA} = 0$ and 1

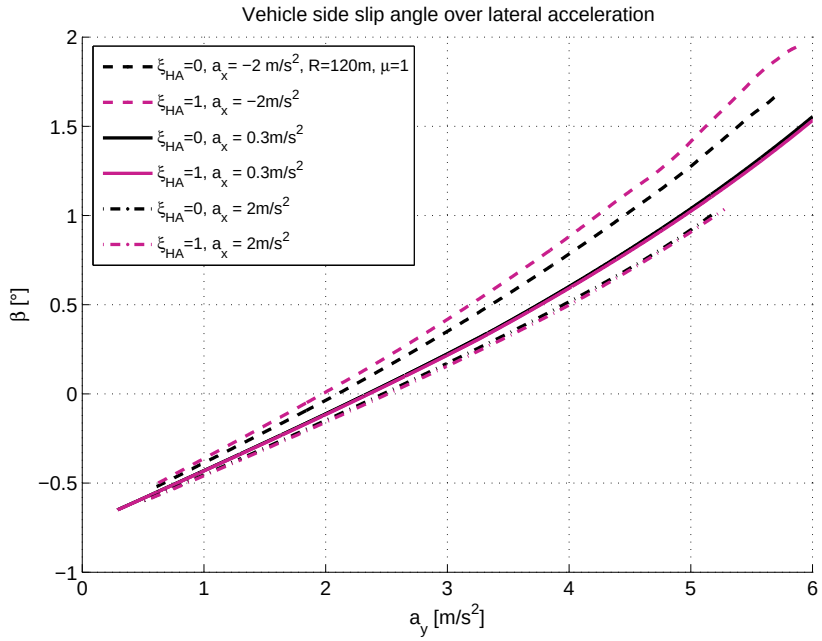

Figure B.2: Vehicle side slip angle versus lateral acceleration for 3 different longitudinal accelerations and $\xi_{HA} = 0$ and 1

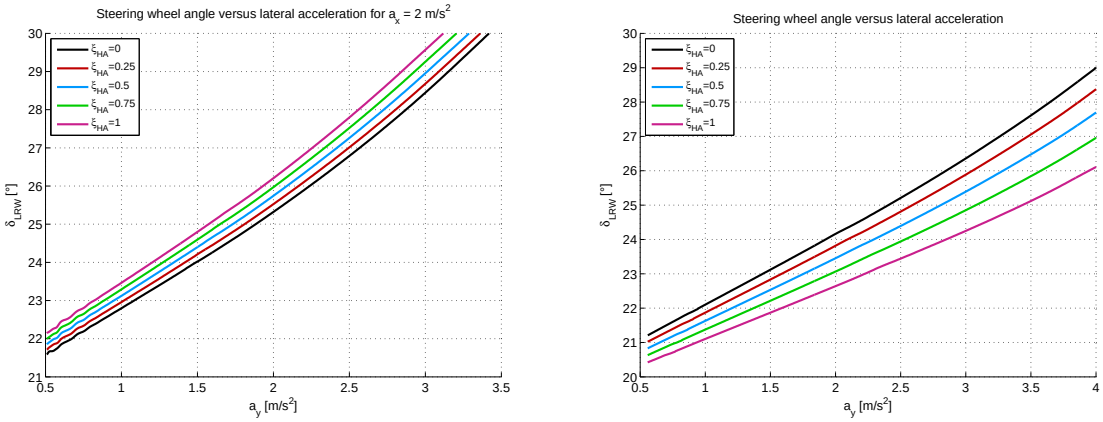

(a) $a_x = 2\,\mathrm{m/s^2}$ (b) $a_x = -2\,\mathrm{m/s^2}$

Figure B.3: Steering wheel angle versus lateral acceleration with different distributions shown for two different longitudinal accelerations a_x

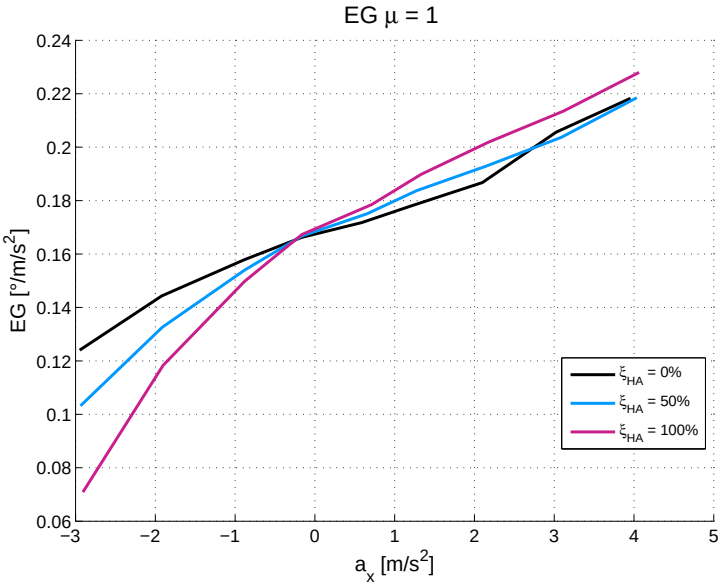

Figure B.4: Difference in understeer gradient versus a_x with different distributions

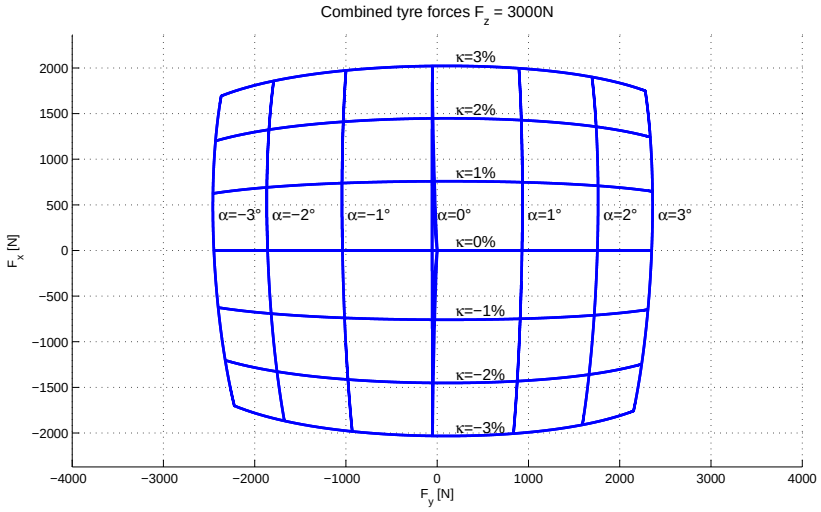

Figure B.5: Friction ellipse for tyre model

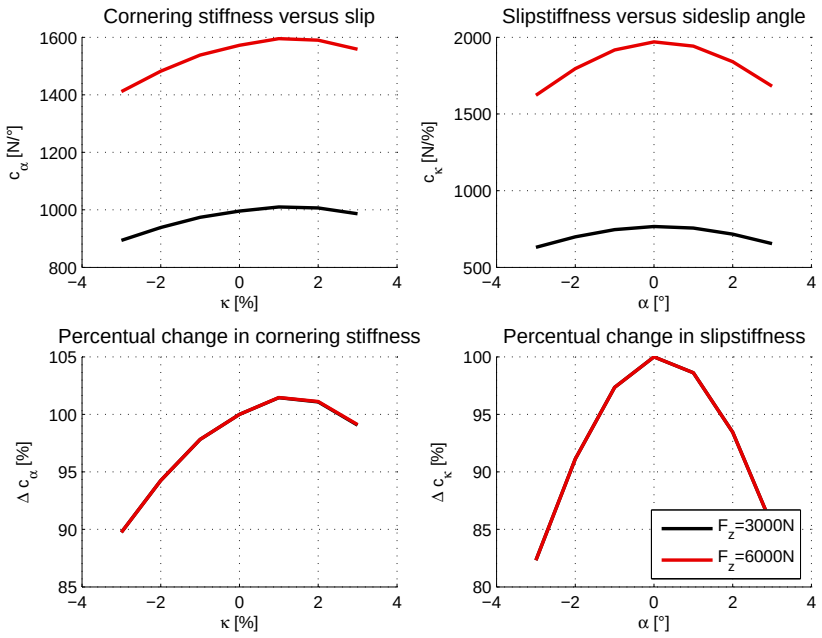

Figure B.6: Stiffnesses and percentual change with respect to longitudinal slip κ and sideslip α

Bibliography

[1] Igo Besselink, *Vehicle Dynamics Lecture Slides*. Eindhoven University of Technology, Eindhoven, 2012.